Characteristic length scale of the intermediate structure in zero-pressure-gradient boundary layer flow

G. I. Barenblatt†, A. J. Chorin†, and V. M. Prostokishin‡

†Department of Mathematics and Lawrence Berkeley National Laboratory, University of California, Evans Hall, Room 970, Berkeley, CA 94720-3840; and ‡P. P. Shirshov Institute of Oceanology, Russian Academy of Sciences, 36 Nakhimov Prospect, Moscow 117218, Russia

Contributed by G. I. Barenblatt, February 10, 2000

In a turbulent boundary layer over a smooth flat plate with zero pressure gradient, the intermediate structure between the viscous sublayer and the free stream consists of two layers: one adjacent to the viscous sublayer and one adjacent to the free stream. When the level of turbulence in the free stream is low, the boundary between the two layers is sharp, and both have a self-similar structure described by Reynolds-number-dependent scaling (power) laws. This structure introduces two length scales: one—the wall-region thickness—determined by the sharp boundary between the two intermediate layers and the second determined by the condition that the velocity distribution in the first intermediate layer be the one common to all wall-bounded flows and in particular coincide with the scaling law previously determined for pipe flows. Using recent experimental data, we determine both these length scales and show that they are close. Our results disagree with the classical model of the "wake region."

Turbulent boundary layer flow over a smooth flat plate outside a close vicinity of the plate tip contains two unambiguous elements: the viscous sublayer adjacent to the plate, where the velocity gradient is large and the viscous stress is comparable with the Reynolds stress, and the statistically uniform free stream.

According to classical theory (1), the region intermediate between these two consists of two layers with different properties. The first, adjacent to the viscous sublayer, is a universal, Reynolds-number-independent logarithmic layer. In the second, the "wake region," there is a smooth transition from the universal logarithmic layer to the free stream.

Our analysis of all available experiments (2–4) contradicts this classical theory. Indeed, in the clear-cut case of a smooth plate and low free stream turbulence, the intermediate structure does consist of two layers. However, the boundary between them is sharp. Most important, both layers are self-similar, substantially Reynolds-number-dependent, and described by different scaling laws. It is interesting to note (see the details below) that the same configuration of two self-similar layers with a sharp interface between them can be seen in all runs used in ref. 1 for the illustration of the wake region model.

We found it possible (2–4) to introduce a characteristic length scale Λ such that the average velocity distribution in the first intermediate layer coincides with Reynolds-number-dependent scaling law obtained previously for pipe flows, when the Reynolds number is chosen as $U\Lambda/\nu$, where U is the free stream velocity and ν is the fluid's kinematic viscosity. The sharp boundary between the self-similar intermediate layers also defines a length scale λ. We show, by analysis of experimental data, that these two length scales λ and Λ are close.

Background. In a previous paper (2), we noted that when the turbulence level in the free stream is small, the intermediate structure between the viscous sublayer and the free stream consists of two self-similar layers: one adjacent to the viscous sublayer where the average velocity profile is described by the scaling law

$$\phi = A\eta^{\alpha} \qquad [1]$$

and one adjacent to the free stream where

$$\phi = B\eta^{\beta}. \qquad [2]$$

Here,

$$\phi = \frac{u}{u_*}, \qquad u_* = \sqrt{\frac{\tau}{\rho}}, \qquad \eta = \frac{u_* y}{\nu}, \qquad [3]$$

u is the average velocity; τ is the shear stress at the wall; ρ and ν are the fluid density and kinematic viscosity; and A, B, α, and β are Reynolds-number-dependent constants.

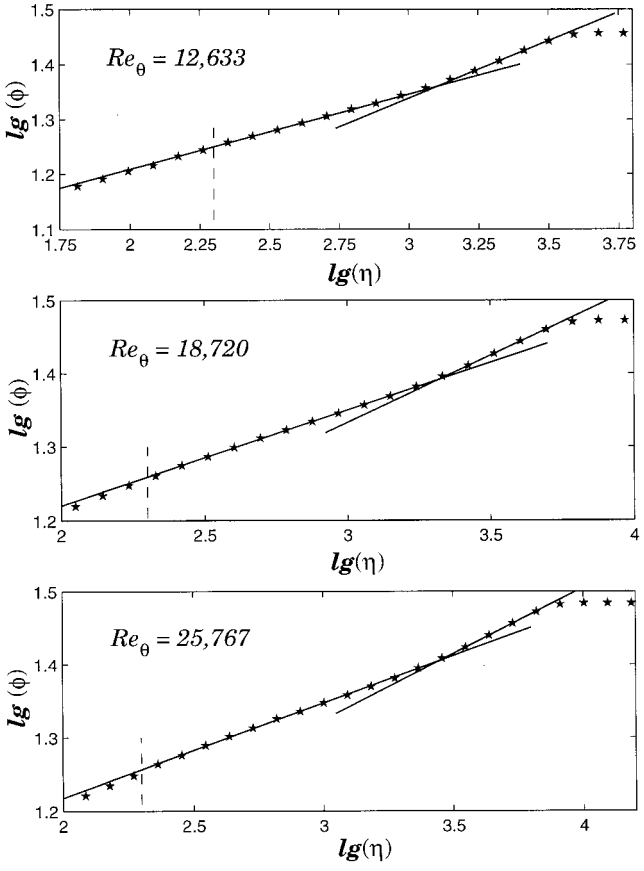

Fig. 1. Examples of Österlund's mean velocity data presented on the internet in bilogarithmic coordinates.

Table 1. Processing of the Österlund data

Re_θ	α	A	β	B	$\ln(Re_1)$	$\ln(Re_2)$	$\ln(Re)$	δ, %	U	u_*	η_*
10,161	0.142	8.43	0.196	5.82	10.27	10.54	10.41	2.5	53.71	1.91	1.0 E+3
10,313	0.140	8.51	0.202	5.53	10.41	10.74	10.58	3.0	37.44	1.33	1.1 E+3
10,386	0.139	8.58	0.204	5.45	10.53	10.81	10.67	2.6	21.21	0.75	1.1 E+3
10,502	0.141	8.38	0.204	5.44	10.18	10.62	10.40	4.2	27.00	0.96	9.9 E+2
11,733	0.139	8.56	0.199	5.57	10.50	10.77	10.63	2.5	42.75	1.50	1.2 E+3
12,150	0.140	8.48	0.199	5.56	10.36	10.69	10.53	3.1	21.42	0.75	1.2 E+3
12,239	0.139	8.55	0.200	5.50	10.47	10.79	10.63	3.0	32.40	1.14	1.3 E+3
12,308	0.137	8.67	0.202	5.46	10.69	10.98	10.83	2.6	21.23	0.74	1.2 E+3
12,633	0.137	8.61	0.209	5.16	10.59	10.96	10.77	3.4	21.42	0.75	1.3 E+3
12,866	0.134	8.88	0.193	5.81	11.05	11.22	11.13	1.5	47.93	1.67	1.3 E+3
12,886	0.137	8.65	0.200	5.52	10.65	10.95	10.80	2.7	26.91	0.94	1.3 E+3
13,878	0.137	8.69	0.196	5.63	10.73	10.99	10.86	2.4	37.74	1.31	1.4 E+3
14,207	0.132	9.01	0.191	5.87	11.28	11.39	11.33	1.0	26.54	0.92	1.4 E+3
14,289	0.132	9.02	0.188	5.98	11.29	11.39	11.34	0.9	53.16	1.84	1.5 E+3
14,972	0.134	8.81	0.198	5.51	10.92	11.16	11.04	2.2	32.37	1.11	1.6 E+3
15,164	0.134	8.80	0.199	5.45	10.91	11.19	11.05	2.6	26.90	0.92	1.5 E+3
15,182	0.130	9.03	0.199	5.45	11.32	11.53	11.42	1.9	26.75	0.92	1.5 E+3
15,512	0.129	9.14	0.189	5.91	11.50	11.61	11.56	1.0	43.02	1.48	1.7 E+3
16,422	0.131	9.08	0.185	6.05	11.39	11.43	11.41	0.3	31.67	1.08	1.8 E+3
17,102	0.134	8.87	0.188	5.91	11.04	11.23	11.13	1.7	37.81	1.29	1.8 E+3
17,279	0.129	9.15	0.187	5.95	11.52	11.62	11.57	0.8	48.37	1.64	1.9 E+3
17,813	0.129	9.11	0.191	5.73	11.45	11.63	11.54	1.6	32.41	1.10	1.9 E+3
17,901	0.135	8.75	0.196	5.51	10.82	11.12	10.97	2.7	32.21	1.09	1.8 E+3
18,479	0.127	9.38	0.178	6.35	11.91	11.85	11.88	0.5	36.74	1.24	2.0 E+3
18,720	0.126	9.34	0.183	6.08	11.85	11.87	11.86	0.2	53.63	1.81	2.0 E+3
19,235	0.126	9.33	0.187	5.89	11.83	11.89	11.86	0.5	43.26	1.46	1.9 E+3
20,258	0.127	9.25	0.188	5.81	11.69	11.80	11.75	0.9	37.40	1.25	2.0 E+3
20,562	0.130	9.08	0.186	5.93	11.40	11.57	11.48	1.5	37.88	1.27	2.0 E+3
20,958	0.125	9.44	0.180	6.16	12.02	12.03	12.02	0.1	48.68	1.63	2.3 E+3
21,099	0.125	9.42	0.180	6.17	11.98	12.00	11.99	0.1	40.00	1.34	2.1 E+3
22,579	0.123	9.54	0.179	6.19	12.19	12.16	12.18	0.3	52.61	1.75	2.4 E+3
22,845	0.126	9.34	0.184	5.95	11.86	11.94	11.90	0.7	42.51	1.41	2.3 E+3
23,119	0.123	9.52	0.177	6.28	12.16	12.15	12.15	0.1	45.35	1.50	2.3 E+3
23,309	0.129	9.11	0.184	5.93	11.44	11.64	11.54	1.7	43.57	1.44	2.3 E+3
23,870	0.121	9.70	0.177	6.30	12.46	12.42	12.44	0.4	46.45	1.53	2.3 E+3
25,767	0.124	9.42	0.181	6.04	11.99	12.08	12.04	0.7	49.11	1.61	2.5 E+3
25,779	0.125	9.30	0.187	5.74	11.79	11.96	11.87	1.5	48.29	1.58	2.7 E+3
26,612	0.120	9.74	0.177	6.24	12.54	12.48	12.51	0.5	52.18	1.71	2.7 E+3
27,320	0.124	9.54	0.173	6.42	12.20	12.13	12.17	0.6	54.04	1.76	3.0 E+3

Our processing of all experimental data available in the literature (3, 4) confirmed these observations and showed that it is always possible to find a length scale Λ such that, setting $Re = U\Lambda/\nu$, we can represent the scaling law of Eq. **1** in the form

$$\phi = \left(\frac{1}{\sqrt{3}}\ln Re + \frac{5}{2}\right)\eta\frac{3}{2\ln Re} \qquad [4]$$

obtained by us earlier for pipe flows (see, e.g., ref. 5). This result suggests that the structure of wall regions in all wall-bounded shear flows at large Reynolds numbers is identical, if the length scale and velocity scale are selected properly. The natural question is, however, what is the physical meaning of this length scale Λ in boundary layer flow? This question is of substantial importance and should be clarified for proper understanding of the identity of scaling laws for different wall-bounded shear flows.

Table 2. Processing of the data used by Coles (1)

No.	α	A	β	B	$\ln(Re_1)$	$\ln(Re_2)$	$\ln(Re)$	δ, %
1	0.163	7.90	0.70	0.42	9.35	9.18	9.27	2
2	0.176	7.29	0.51	0.82	8.30	8.55	8.43	3
3	0.180	7.17	0.56	0.66	8.09	8.34	8.22	3
4	0.171	7.43	0.57	0.60	8.55	8.75	8.65	3
5	0.185	6.77	0.64	0.30	7.41	8.11	7.76	9
6	0.151	8.20	0.55	0.49	9.87	9.96	9.92	1
7	0.158	7.71	0.50	0.67	9.02	9.52	9.27	6

We note that the intermediate structure has another characteristic length scale λ—the wall-region thickness—determined by the sharp intersection $\eta = \eta_*$ of the two velocity distribution laws $\phi = A\eta^\alpha$ and $\phi = B\eta^\beta$ valid in the different layers. We have

$$A\eta_*^\alpha = B\eta_*^\beta, \qquad [5]$$

such that

$$\eta_* = \left(\frac{A}{B}\right)^{\frac{1}{\beta-\alpha}}, \qquad [6]$$

and the wall-region thickness λ is determined by the relation

$$\lambda = \left(\frac{A}{B}\right)^{\frac{1}{\beta-\alpha}}\frac{\nu}{u_*}. \qquad [7]$$

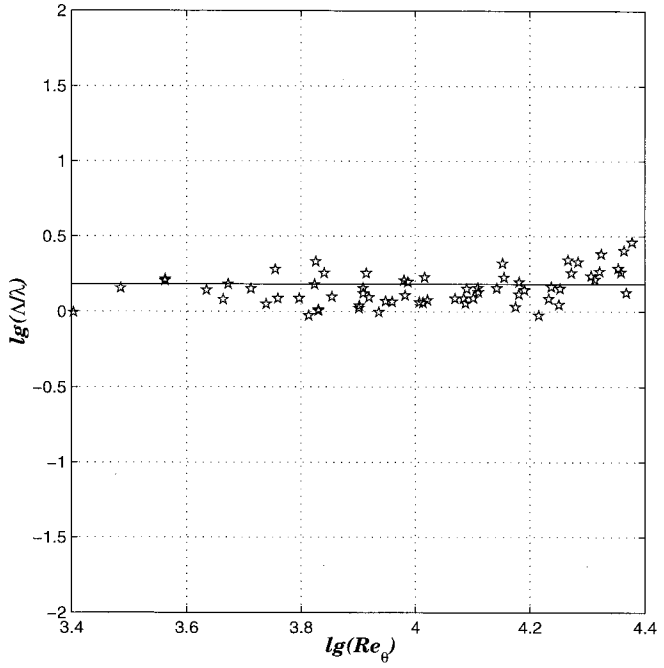

Fig. 2. The logarithm of the ratio of length scales Λ and λ for various Re_θ obtained by processing Österlund's mean velocity data presented on the internet.

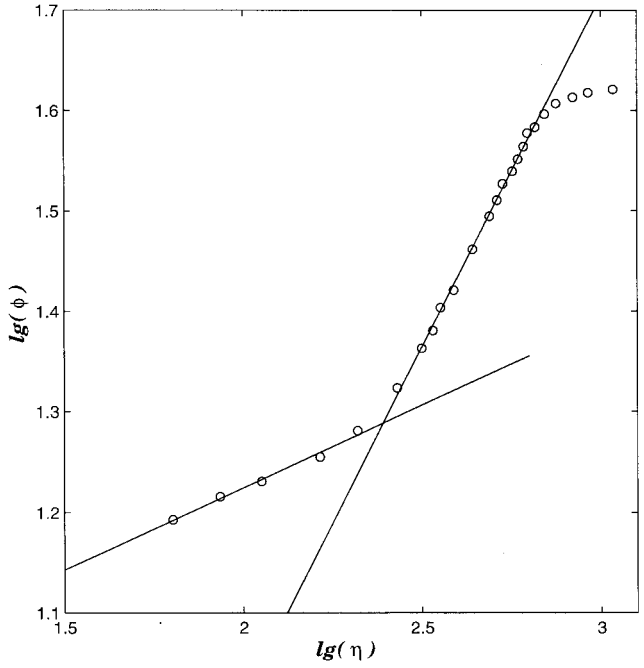

Fig. 3. Example of mean velocity data of Klebanoff and Diehl, presented in ref. 1, in bilogarithmic coordinates.

On the other hand, the characteristic length scale Λ is determined by the relation

$$\Lambda = Re\frac{\nu}{U} = \left(\frac{u_*}{U}\right)\left(\frac{\nu}{u_*}\right)Re\,, \qquad [8]$$

such that the ratio of these two scales is

$$\frac{\Lambda}{\lambda} = \left(\frac{u_*}{U}Re\right)\frac{1}{\eta_*} = \left(\frac{u_*}{U}Re\right)\left(\frac{B}{A}\right)^{\frac{1}{\beta-\alpha}}. \qquad [9]$$

Analysis of Experimental Data. We analyzed the recent data of J. M. Österlund presented on the internet (www.mesh.kth.se/~jens/zpg/). The data seem to us to be reliable, however much we disagree with the processing and interpretation in the paper by Österlund *et al*. (ref. 6; see also ref. 4). All 70 runs presented on the internet give the characteristic broken-line average velocity distribution in lg η, lg ϕ coordinates (see the examples in Fig. 1; all of the other cases are similar), such that the possibility of determining A, α, B, β, and η_* accurately from these experimental data is unquestionable. These results are presented in Table 1 for all of Österlund's experiments where $Re_\theta = U\theta/\nu > 10{,}000$. Here, θ is the momentum thickness; the runs in the Österlund's experimental data are labeled by Re_θ. The effective Reynolds number Re was obtained (4) by the formula

$$\ln Re = \frac{1}{2}(\ln Re_1 + \ln Re_2), \qquad [10]$$

where $\ln Re_1$ and $\ln Re_2$ are the solutions of the equations

$$\frac{1}{\sqrt{3}}\ln Re_1 + \frac{5}{2} = A, \qquad \frac{3}{2\ln Re_2} = \alpha, \qquad [11]$$

and the values of A and α were obtained by standard statistical processing of Österlund's data. For $Re_\theta > 10{,}000$, the difference δ between $\ln Re_1$ and $\ln Re_2$ does not exceed 3%, such that they coincide within experimental accuracy.
According to Eqs. **8** and **9**,

$$\lg\frac{\Lambda}{\lambda} = (\lg Re - \lg\eta_*) + \lg\frac{u_*}{U}. \qquad [12]$$

The data for u_* and U are presented by Österlund on the internet for each run. In Fig. 2, we present the values of $\lg(\Lambda/\lambda)$ for all runs. The mean value of $\lg(\Lambda/\lambda)$ is approximately 0.2, such that the characteristic length scale Λ is about 1.6 times the thickness of the wall region.

If we take into account that Λ is calculated from the value of Re and that $\ln Re$, not Re itself, has been determined from experiment, the ratios Λ/λ as shown in Fig. 2 are close to 1.5.

We processed in refs. 3 and 4 the data of 90 zero-pressure-gradient boundary layer experiments at low free stream turbulence performed by different authors during the last 25 years—all of the experiments of this kind available to us. Without exception, all runs revealed identical configurations of the intermediate structure in the boundary layer: two adjacent self-similar layers separated by a sharp interface.

According to the classical model (1), the intermediate structure consists of the (universal) logarithmic layer and a non-self-similar wake region smoothly matching the logarithmic layer. It was natural to process also the very data used in ref. 1 for the justification of the wake region model with the general procedure we used on the other data. The data presented in figure 21 of ref. 1 were scanned and replotted in lg η, lg ϕ coordinates as was done for all experimental data processed in refs. 3 and 4. Processing revealed the same broken-line structure, i.e., two adjacent self-similar layers (see Table 2 and Fig. 3, where a typical example is presented). The difference between $\ln Re_1$ and $\ln Re_2$ determined from the wall layer data is small: this result shows that the procedure is adequate. We conjecture that the

values of β are larger than those in newer experiments because of a nonzero pressure gradient in all these runs (see ref. 1). The results of our processing fail to confirm the wake region model proposed in ref. 1.

Conclusions. We have shown that one can find a length scale Λ, such that, if the Reynolds number Re in a zero-pressure-gradient boundary layer flow is defined by $Re = U\Lambda/\nu$, where U is the free stream velocity and ν is the kinematic viscosity, then the scaling law for the self-similar region adjacent to the viscous sublayer coincides with the scaling law for turbulence pipe flow. Using the recent experimental data of Österlund (www.mesh.kth.se/~jens/zpg/), we confirmed this fact and reached the important conclusion that Λ is about 1.6 times the wall-region thickness. Our results are in disagreement with the classical model of the wake region in the boundary layer (1).

This work was supported in part by the Applied Mathematics subprogram of the U.S. Department of Energy under Contract DE-AC03-76-SF00098 and in part by National Science Foundation Grants DMS 94-16431 and DMS 97-32710.

1. Coles, D. (1956) *J. Fluid Mech.* **1,** 191–226.
2. Barenblatt, G. I., Chorin, A. J., Hald, O. & Prostokishin, V. M. (1997) *Proc. Natl. Acad. Sci. USA* **94,** 7817–7819.
3. Barenblatt, G. I., Chorin, A. J. & Prostokishin, V. M. (2000) *J. Fluid Mech.* **400,** 1–21.
4. Barenblatt, G. I., Chorin, A. J. & Prostokishin, V. M. (2000) *Analysis of Experimental Investigations of Self-Similar Structures in Zero-Pressure-Gradient Boundary Layers at Large Reynolds Numbers* (Center for Pure and Applied Mathematics, Univ. of California, Berkeley, CA), report CPAM 777.
5. Barenblatt, G. I., Chorin, A. J. & Prostokishin, V. M. (1997) *Appl. Mech. Rev.* **50,** 413–429.
6. Österlund, J. M., Johansson, A. V., Nagib, H. M. & Hites, M. H. (2000) *Phys. Fluids* **12,** 1–4.